

Density Functional Study of Protonated Formylmetallocenes

Andela Šarić,[#] Valerije Vrčec,^{*†} and Michael Bühl^{*‡§¶}

Faculty of Sciences, University of Zagreb, HR-10000, Zagreb, Croatia, Faculty of Pharmacy and Biochemistry, University of Zagreb, HR-10000, Zagreb, Croatia, and Max-Planck-Institut für Kohlenforschung, Kaiser-Wilhelm-Platz 1, D-45470 Mülheim an der Ruhr, Germany

Received September 14, 2007

Protonated formylmetallocenes $[M(C_5H_5)(C_5H_4-CHOH)]^+$ ($M = Fe, Ru$) and their isomers have been studied at the BP86 and B3LYP levels of density functional theory. Oxygen-protonated isomers are the most stable forms in each case, with a plethora of ring- or metal-protonated species at least ca. 14 and 10 kcal/mol higher in energy for $M = Fe$ and Ru , respectively. The computed rotational barriers around the C–C bond connecting the cyclopentadienyl and protonated formyl moieties, ca. 18 kcal/mol, are indicative of substantial conjugation between these moieties. Some of the ring- and iron-protonated species are models for possible intermediates in Friedel–Crafts acylation of ferrocene, and the computations provide further evidence that *exo* attack is clearly favored over *endo* attack of the electrophile in this reaction. The structures of the most stable mono- and diprotonated formylferrocenes are corroborated by the good agreement between GIAO-B3LYP-computed and experimental NMR chemical shifts.

1. Introduction

Electrophilic substitutions at ferrocene are textbook examples¹ of organometallic reactions. Protonated ferrocene, a product of the reaction with the simplest electrophile, has been studied extensively, both experimentally and computationally.² In comparison, the chemistry involved in protonation of substituted ferrocenes is known in less detail. It has been shown experimentally that the protonation of both acylferrocenes $[FcCOR, Fc = Fe(C_5H_5)(C_5H_4)]$ ^{3,4} and ferrocenyl ethers $[Fc(CH_2)_nOR]$ ⁵ results in the formation of the corresponding stable protonated species. On the basis of spectroscopic evidence,^{4,5} the site of protonation was found at the carbonyl and ether oxygen atoms, respectively.

Protonated ferrocene-containing aldehydes can undergo acyl group elimination, which results in formation of ferrocene and acylium cations. This process has important implications for the Friedel–Crafts acylation of ferrocene, formally the reverse reaction. However, only little is known about the precise mechanism of the corresponding processes. There is experimental⁶ and computational⁷ evidence that the electrophile in the acylation process attacks one of the Cp rings in an *exo* fashion, rather than via an *endo* pathway with possible metal involvement. These computations were performed at the lowest

level of density functional theory (DFT), however, and only for selected minima. We now present an extensive DFT study of protonated formylferrocene, including careful conformational analysis in order to identify the most stable form within each family of minima. Activation barriers for interconversion of selected isomers are also reported. A detailed mechanistic knowledge of these processes could provide more information on reactions (substitutions, eliminations) with ferrocene derivatives involving carbocation intermediates and could help in better design of new ferrocene analogues and shed light on many questions regarding polymerization of ferrocene-stabilized carbocations.

Carbonyl groups are synthons to access almost any conceivable structure and functionality, and for that reason formylated ferrocene (Fc-CHO) and ruthenocene (Rc-CHO) are of fundamental and practical interest. A series of biologically active compounds and derivatives with potential technological applications were prepared using both Fc-CHO and Rc-CHO as precursors or intermediates in corresponding syntheses.⁸ These formylated metallocenes have also been found as interesting model compounds in organometallic biochemistry, as they are involved in reactions with enzymes and proteins.⁹ Reaction of formylferrocene with an organozinc reagent can be turned into an asymmetric autocatalytic process,¹⁰ another fascinating area of chemistry.

In many of these reactions, the carbonyl species may interact with Lewis acids or hydrogen-bond donors, which can activate these compounds and make them more susceptible to versatile transformation processes. This aspect provides further motiva-

* Corresponding authors. E-mail: valerije@pharma.hr; buehl@mpi-muelheim.mpg.de.

[#] Faculty of Sciences, University of Zagreb.

[†] Faculty of Pharmacy and Biochemistry, University of Zagreb.

[‡] Max-Planck-Institut für Kohlenforschung.

[§] Present address: School of Chemistry, North Haugh, University of St. Andrews, St. Andrews, Fife KY16 9ST, UK.

(1) Eilschenbroich, C. *Organometallics*, 3rd ed.; Wiley-VCH: Weinheim, 2006.

(2) Bühl, M.; Grigoleit, S. *Organometallics* **2005**, *24*, 1516–1527 and references cited therein.

(3) Neshvad, G.; Roberts, R. M. G.; Silver, J. J. *Organomet. Chem.* **1982**, *236*, 349–358.

(4) Olah, G. A.; Mo, Y. K. *J. Organomet. Chem.* **1973**, *60*, 311–321.

(5) Olah, G. A. *J. Am. Chem. Soc.* **1992**, *114*, 1097–1098.

(6) See e.g.: Cunningham, A. F., Jr. *J. Am. Chem. Soc.* **1991**, *113*, 4864–4870.

(7) Mayor-Lopez, M. J.; Weber, J.; Mannfors, B.; Cunningham, A. F., Jr. *Organometallics* **1998**, *17*, 4983–4991.

(8) (a) Sato, M.; Nagata, T.; Tanemura, A.; Fujihara, T.; Kumakura, S.; Unoura, K. *Chem.—Eur. J.* **2004**, *10*, 2166–2178. (b) Beagly, P.; Blackie, M. A. L.; Chibale, K.; Clarkson, C.; Meijboom, R.; Moss, J. R.; Smith, P. J.; Su, H. *Dalton Trans.* **2003**, 3046–3051. (c) Maricic, S.; Freijid, T. J. *Org. Chem.* **2002**, *67*, 7600–7606. (d) Burrell, A. K.; Campbell, W. M.; Officer, D. L.; Scott, S. M.; Gordon, K. C.; McDonald, M. R. *J. Chem. Soc., Dalton Trans.* **1999**, 3349–3354.

(9) Ryabov, A. D. *Angew. Chem., Int. Ed. Engl.* **1991**, *30*, 931–941.

(10) (a) Soai, K.; Hayase, T.; Takai, K. *Tetrahedron: Asymmetry* **1995**, *6*, 637–638. (b) Soai, K.; Shibata, T.; Sato, K. *Acc. Chem. Res.* **2000**, *33*, 382–390.

tion to study the protonation of these metallocene-containing aldehydes and the detailed mechanism underlying it, as this reaction can be viewed as an activation taken to the extreme.

2. Computational Details

Geometries were fully optimized (in specified symmetry) at the RI-BP86 level as implemented in the G03 program,¹¹ employing the exchange and correlation functionals of Becke¹² and Perdew,¹³ respectively, together with a fine integration grid (75 radial shells with 302 angular points per shell), the augmented Wachters' basis¹⁴ on Fe (8s7p4d), 6-31G* basis¹⁵ on all other elements, and 6-31G** on the extra protons, denoted AE1^(*), and suitable auxiliary basis sets for the fitting of the Coulomb potential.¹⁶ For Ru, the Stuttgart–Dresden relativistic effective core potential and the corresponding [6s5p3d] valence basis¹⁷ have been employed, denoted ECP1^(*). This and comparable DFT levels have proven quite successful for transition-metal compounds and are well suited for the description of structures, energies, vibrational frequencies, and other properties.¹⁸ Harmonic frequencies were computed from analytical second derivatives.

Natural population analyses and topological (Bader) analyses¹⁹ of the RI-BP86 total electron densities have been performed using the NBO²⁰ routines in Gaussian 03 and the Morphy program,²¹ respectively.

Magnetic shieldings (σ) were computed at the B3LYP²² level for the RI-BP86 equilibrium geometries, employing GIAOs (gauge-including atomic orbitals)²³ and basis II', i.e., the augmented Wachters basis¹⁴ on Fe, IGLO-basis II,²⁴ which is essentially of polarized triple- ζ quality, on C and O, and IGLO-DZ basis²⁴ on

hydrogen. Chemical shifts were calculated relative to ferrocene (⁵⁷Fe, ¹³C, and ¹H magnetic shieldings –4372.8, 106.2, and 28.1 ppm at the same level), and the ¹³C, ¹H, and ⁵⁷Fe chemical shifts were converted to the usual standards, TMS and Fe(CO)₅, using the experimental $\delta(^{13}\text{C})$, $\delta(^1\text{H})$, and $\delta(^{57}\text{Fe})$ values of ferrocene, 67.8, 4.2, and 1532 ppm, respectively.²⁵ This level has been shown to perform very well for transition-metal chemical shifts, including ⁵⁷Fe, where further enlargement of the basis set in the NMR part has afforded only minor changes in the computed values.²⁶

For structures **1a**, **1b**, **3a**, **5a**, and **9a** (M = Fe) single-point energy calculations were performed at the BP86/AE1^(*) level employing the polarizable continuum model (PCM) of Tomasi and co-workers²⁷ (using the parameters of water, UFF radii from the united atom topological model with an additional sphere on the extra proton).

3. Results and Discussion

3.1. Carbonyl-Protonated Forms of Formylmetallocenes.

As expected, the carbonyl-protonated structures (**1a** and **1b**) are the most stable protonated forms of formylmetallocenes (Scheme 1, M = Fe or Ru). In the case of the protonated formylferrocene both the ring- (**3–8**) and metal-protonated forms (**9–11**) were found ca. 15 kcal/mol less stable (see below).²⁸ Similar results are obtained for protonated formylruthenocene. Ring-protonated forms of formylruthenocene (**3–6**) converged, during geometry optimizations, to the more stable metal-protonated forms, except the C1-protonated structures with the formyl group oriented orthogonal to the cyclopentadiene ring (**7**, **8**). However, the exact nature of these stationary points (**7**, **8**, M = Ru) at the corresponding potential energy surface is somewhat controversial, as discussed later.

Two different forms of carbonyl-protonated formylmetallocenes were located as minima, i.e., **1a** and **1b** isomers (the proton is either *cis* or *trans* to the methine hydrogen, respectively), the former being more stable by 0.6 kcal/mol (M = Fe) or 0.7 kcal/mol (M = Ru). The same ordering is found for the respective *cis* and *trans* rotamers of protonated benzaldehyde (the former is calculated more stable than the latter by ca. 2 kcal/mol), which is in agreement with experimental observations that *cis* isomeric carboxonium ions are generally more stable than *trans* isomers.²⁹

Formally, **1a** and **1b** can be described as carbocations CHR₁R₂⁺ (cf. structure A in Scheme 2), stabilized by conjugation with a p-type lone pair from a hydroxy substituent and with the π -system from a metallocenyl moiety (cf. limiting resonance structures B and C, respectively, in Scheme 2). The limiting structure C is formally a pentafulvene complex, for which it is known that the α -carbon is bent downward from the Cp plane toward the metal center.³⁰ The calculated angle (BP86 level) of the C1–C(carbonyl) bond with the Cp plane is

(11) Frisch, M. J.; Trucks, G. W.; Schlegel, H. B.; Scuseria, G. E.; Robb, M. A.; Cheeseman, J. R.; Montgomery, J. A., Jr.; Vreven, T.; Kudin, K. N.; urant, J. C.; Millam, J. M.; Iyengar, S. S.; Tomasi, J.; Barone, V.; Mennucci, B.; Cossi, M.; Scalmani, G.; Rega, N.; Petersson, G. A.; Nakatsuji, H.; Hada, M.; Ehara, M.; Toyota, K.; Fukuda, R.; Hasegawa, J.; Ishida, M.; Nakajima, T.; Honda, Y.; Kitao, O.; Nakai, H.; Klene, M.; Li, X.; Knox, J. E.; Hratchian, H. P.; Cross, J. B.; Adamo, C.; Jaramillo, J.; Gomperts, R.; Stratmann, R.; Yazyev, O.; Austin, A. J.; Cammi, R.; Pomelli, C.; Ochterski, J. W.; Ayala, P. Y.; Morokuma, K.; Voth, G. A.; Salvador, P.; Dannenberg, J. J.; Zakrzewski, V. G.; Dapprich, S.; Daniels, A. D.; Strain, M. C.; Farkas, O.; Malick, D. K.; Rabuck, A. D.; Raghavachari, K.; Foresman, J. B.; Ortiz, J. V.; Cui, Q.; Baboul, A. G.; Clifford, S.; Cioslowski, J.; Stefanov, B. B.; Liu, G.; Liashenko, A.; Piskorz, P.; Komaromi, I.; Martin, R. L.; Fox, D. J.; Keith, T.; Al-Laham, M. A.; Peng, C. Y.; Nanayakkara, A.; Challacombe, M.; Gill, P. M. W.; Johnson, B.; Chen, W.; Wong, M. W.; Gonzalez, C.; Pople, J. A. *Gaussian 03*; Gaussian, Inc.: Pittsburgh, PA, 2003.

(12) Becke, A. D. *Phys. Rev. A* **1988**, *38*, 3098–3100.

(13) (a) Perdew, J. P. *Phys. Rev. B* **1986**, *33*, 8822–8824. (b) Perdew, J. P. *Phys. Rev. B* **1986**, *34*, 7406.

(14) (a) Wachters, A. J. H. *J. Chem. Phys.* **1970**, *52*, 1033–1036. (b) Hay, P. J. *J. Chem. Phys.* **1977**, *66*, 4377–4384.

(15) (a) Hehre, W. J.; Ditchfield, R.; Pople, J. A. *J. Chem. Phys.* **1972**, *56*, 2257–2261. (b) Hariharan, P. C.; Pople, J. A. *Theor. Chim. Acta.* **1973**, *28*, 213–222.

(16) Generated automatically according to the procedure implemented in Gaussian 03.

(17) Andrae, D.; Häussermann, U.; Dolg, M.; Stoll, H.; Preuss, H. *Theor. Chim. Acta* **1990**, *77*, 123–141.

(18) See for instance: Koch, W.; Holthausen, M. C. *A Chemist's Guide to Density Functional Theory*; Wiley-VCH: Weinheim, 2000, and the extensive bibliography therein.

(19) Bader, R. F. W. *Atoms in Molecules*; Oxford Press: New York, 1990.

(20) Reed, A. E.; Curtiss, L. A.; Weinhold, F. *Chem. Rev.* **1988**, *88*, 899–926.

(21) Popelier, P. L. A. *Comput. Phys. Commun.* **1996**, *93*, 212–240.

(22) Lee, C.; Yang, W.; Parr, R. G. *Phys. Rev. B* **1988**, *37*, 785–789.

(23) (a) Ditchfield, R. *Mol. Phys.* **1974**, *27*, 789–807. (b) Wolinski, K.; Hinton, J. F.; Pulay, P. *J. Am. Chem. Soc.* **1990**, *112*, 8251–8260. GIAO-DFT implementation: (c) Cheeseman, J. R.; Trucks, G. W.; Keith, T. A.; Frisch, M. J. *J. Chem. Phys.* **1996**, *104*, 5497–5509.

(24) Kutzelnigg, W.; Fleischer, U.; Schindler, M. In *NMR Basic Principles and Progress*; Springer-Verlag: Berlin, 1990; Vol. 23, pp 165–262.

(25) For experimental ⁵⁷Fe NMR data: Haslinger E.; Robin W.; Schloegel K.; Weissensteiner W. *J. Organomet. Chem.* **1981**, *218*, C11. For experimental ¹³C and ¹H NMR data: Spectral Database for Organic Compounds SDBS, accessed at <http://riodb.ibase.aist.go.jp>.

(26) Bühl, M. *Chem. Phys. Lett.* **1997**, *267*, 251–257.

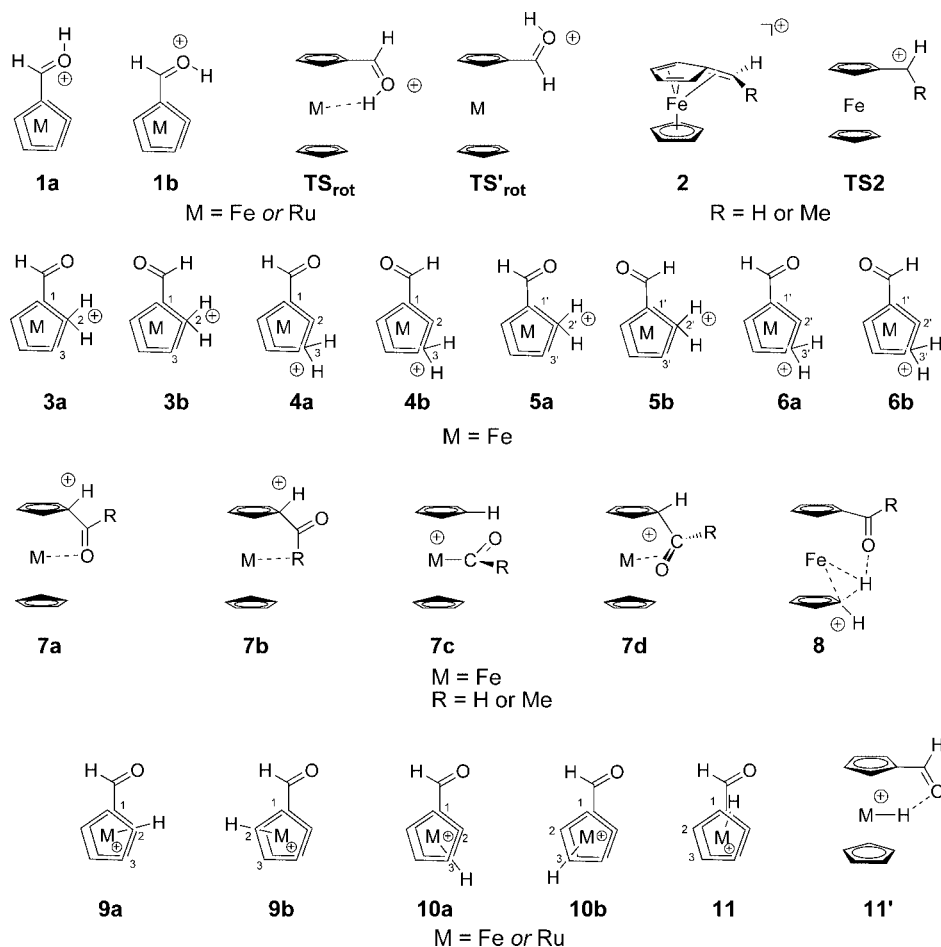
(27) (a) As implemented in G03: Barone, V.; Cossi, M.; Tomasi, J. *J. Comput. Chem.* **1998**, *19*, 404–417. (b) Cossi, M.; Scalmani, G.; Rega, N.; Barone, V. *J. Chem. Phys.* **2002**, *117*, 43–54. (c) Cossi, M.; Crescenzi, O. *J. Chem. Phys.* **2003**, *19*, 8863–8872.

(28) Relative energy differences were not influenced by modeling solvent in PCM calculations, except the *trans*-isomer **1b** is calculated to be 1.8 kcal/mol less stable than the *cis*-isomer **1a**, which is 1.2 kcal/mol larger than that calculated in the gas phase (see Supporting Information).

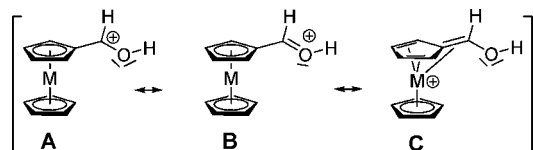
(29) Olah, G. A.; Rasul, G.; York, C.; Prakash, G. K. S. *J. Am. Chem. Soc.* **1995**, *117*, 11211–11214.

(30) Gleiter, R.; Bleiholder, C.; Rominger, F. *Organometallics* **2007**, *26*, 4850–4859, and references therein.

Scheme 1



Scheme 2



155.2° (**1a**, $M = \text{Fe}$), which is, indeed, similar to the corresponding angle (143.6°) calculated for the ferrocenylalkylium ion FcCHMe^+ , **2** (see below, Scheme 1).

The relative strength of the stabilizing interactions in structures B and C can be conveniently assessed by the barriers for rotation about the corresponding C–O or C–C bonds. The barrier for rotation about the C–O bond, a process interconverting **1a** and **1b**, is calculated to be 9.1 kcal/mol for $M = \text{Fe}$ (Table 1).³¹ In the corresponding transition state structure **TS_{1a,b}**, the O–H bond is perpendicular to the plane of the carbonyl group and is situated in *exo* position relative to the ferrocenyl moiety. The other transition state structure **TS'_{1a,b}** for the same **1a** → **1b** interconversion, with the O–H bond in *endo* position, is computed 1.1 kcal/mol higher in energy for $M = \text{Fe}$. Similar results were obtained for the carbonyl-protonated formylru-

thenocene, where the rotational barriers via **TS_{1a,b}** and **TS'_{1a,b}** are 6.4 and 8.2 kcal/mol, respectively (Table 1).

Interestingly, the calculated energy barrier for the *cis*–*trans* isomerization process in protonated benzaldehyde, where no metal participation is possible, is much higher (15.1 kcal/mol, BP86/AE1^(*) level) than the corresponding calculated energy barriers in protonated formylmetallocenes (9.1 and 6.4 kcal/mol for $M = \text{Fe}$ and Ru, respectively). These results suggest that the metal strongly influences this isomerization process.

For the rotation of the protonated formyl group about the C1–C(carbonyl) bond in formylmetallocenes, which effectively “shuts off” conjugation between the carbocationic moiety and the metallocene (via C in Scheme 2), two different transition states can be located, **TS_{rot}** and **TS'_{rot}** (Scheme 1). The former is stabilized by an intramolecular interaction between the metal d-orbitals and the H atom of the protonated carbonyl group, reminiscent of that in ferrocene-containing alcohols.³² The resulting rotational barriers are 17.8 and 17.9 kcal/mol for $M = \text{Fe}$ and Ru, respectively.³³ The transition states **TS'_{rot}** ($M = \text{Fe or Ru}$), where no such interactions are possible, are significantly higher in energy, 22.0 and 26.1 kcal/mol above **1a** for $M = \text{Fe}$ and Ru, respectively. These values are quite similar to the corresponding calculated barrier in protonated benzaldehyde (22.7 kcal/mol) and are much higher than those

(31) It should be noted that there is still p-conjugation between C and O in this perpendicular arrangement, namely involving the sp^2 - rather than the p-type lone pair on the O atom. For the protonated formaldehyde parent, this interaction is so strong that a linear COH arrangement ensues (under rehybridization of the O atom to sp). Thus, a rotated H_2COH^+ in C_s symmetry optimizes to a C_{2v} -symmetric structure at BP86, in agreement with earlier ab initio computations; see for example: Kapp, J.; Schade, C.; El-Nahsa, A. M.; Schleyer, P. v. R. *Angew. Chem., Int. Ed. Engl.* **1996**, *35*, 2236–2238.

(32) This interaction has recently been counted among the “diverse world of unconventional hydrogen bonds”; see: Belkova, N. V.; Shubina, E. S.; Epstein, L. M. *Acc. Chem. Res.* **2005**, *38*, 624–631.

(33) The corresponding transition state structures **TS_{rot}** and **TS'_{rot}**, where two hydrogen atoms of the protonated formyl group are in *cis* position, were calculated 2–3 kcal/mol higher in energy.

Table 1. Relative Energy Differences (in kcal/mol) for Metallocene Structures Discussed in this Work

structure	M = Fe		M = Ru	
	ΔE BP86/AE1 ^(*)	ΔE B3LYP/AE1 ^(*)	ΔE BP86/ECPI ^(*)	ΔE B3LYP/ECPI ^(*)
1a	0	0	0	0
1b	0.6	0.9	0.6	0.9
3a	14.5	15.5		
3b	15.3	17.1		
4a	16.1	17.9		
4b	15.7	17.2		
5a	15.0	15.9		
5b	15.1	16.2		
6a	16.0	16.5		
6b	15.5	16.3		
7a	16.7	15.5	12.9 ^a	12.8 ^a
7b	34.3	35.7	30.1 ^a	32.6 ^a
7c	18.1	23.6	12.4	14.1
7d	29.1	28.7	25.0	26.1
8	16.1	17.0		
9a	14.4		9.6	10.2
9b	14.8		9.7	10.3
10a	15.7		10.9	11.3
10b	15.1		10.2	10.6
11			12.4	12.9
11'	19.2 ^b	23.2 ^b	12.1	13.6
TS_{1a_b}	9.1	8.9	6.4	6.4
TS'_{1a_b}	10.2	11.2	8.2	8.3
TS_{rot}	17.8	21.3	17.9	21.5
TS'_{rot}	22.0	25.3	26.1	28.9
TS_{11'_1b}			17.0	20.0

^a A structure not located as a minimum with higher basis set (6-311 + G**) or better grid size (ultrafine). ^b Transition state structure (NImag = 1).

for the rotation about the C–O bonds discussed above. This finding suggests that conjugation from the π -ligand (via C in Scheme 2) is more important than that from the oxygen lone pair (via B in Scheme 2).

The extent of the apparent metal participation in stabilizing the transition states **TS_{rot}** is noteworthy (ca. 5–8 kcal/mol with respect to **TS'_{rot}**), as it exceeds that in ferrocenylmethanol, FcCH₂OH, where it amounts to 1–2 kcal/mol.³⁴ This stabilizing interaction in **TS_{rot}** was further investigated by computing Wiberg bond indices (WBIs)³⁵ and by performing topological (Bader) analysis of the total electron density. For M = Fe no bond critical point (BCP) or atomic bond path between the metal and the proton is found, suggesting that the interaction between the two atoms is mainly electrostatic in nature. For M = Ru, topological analysis confirms the presence of a bond path and a BCP between both atoms ($\rho = 0.031$ au, $\nabla^2\rho = 0.032$ au), suggesting that normal hydrogen bonding between Ru and H is operative.

These findings were further supported by the WBIs derived from NBO analysis, which are a measure for the covalent contributions to a given bond. At the BP86/AE1^(*) or BP86/ECPI^(*) levels, the calculated WBIs between the metal and the proton in **TS_{rot}** are 0.014 and 0.087 for M = Fe and Ru, respectively. The WBI between the iron center and hydroxyl hydrogen in ferrocenylmethanol is only 0.002.³⁴ The corresponding value for **TS_{rot}** (M = Fe) is calculated to be 7 times larger, indicating a much stronger interaction between the metal and the hydrogen atom. An even larger WBI is calculated for the Ru congener, consistent with the hydrogen bonding between ruthenium and hydrogen atoms emerging from the topological analysis.³⁶

These results are in agreement with the earlier observation that the critical distance of 2.3–2.5 Å between the metal and proton in metallocenes is necessary for a stronger electrostatic interaction or for hydrogen bonding between the metal and proton to be operative.³⁴ In the case of **TS_{rot}** (M = Fe) this distance was calculated to be 2.61 Å, slightly above the 2.5 Å threshold necessary for hydrogen bonding to be operative, while in the case of **TS_{rot}** (M = Ru) it is found to be 2.35 Å, i.e., well within the proposed critical distance range.

Rotation of the protonated formyl group around the C1–C(carbonyl) bond in **1a** and **1b** isomers of metallocenes is severely hindered as compared to the corresponding formyl group rotation in neutral forms.^{37,38} There are several examples of restricted rotation in metallocenyl ions;³⁹ however only in one case has the energy barrier been determined experimentally, namely, for the ferrocenylalkylium ion FcCHR⁺ **2** (Scheme 1, R = Me).⁴⁰ In this system, the electrostatic interaction between metal and hydrogen atoms in the corresponding transition structure **TS2** should be much weaker. In fact, a rotational barrier of ca. 25 kcal/mol has been determined for this system,⁴⁰ much higher than for the corresponding process in **1b** (M = Fe) via **TS_{rot}**. The experimental value for **2** (R = Me) is reasonably well reproduced at BP86/AE1^(*) and B3LYP/AE1^(*) levels (computed barriers are 29.0 and 26.5 kcal/mol, respectively) and is similar to the barrier in **1b** via **TS'_{rot}**, which also lacks stabilization by a Fe···H interaction.

To summarize this part, rotation about the C–O bond in protonated formylmetallocenes is much more facile than that about C1–C(carbonyl) bonds, even if in the latter case (specifically in **TS_{rot}**) the energy penalty due to loss of resonance energy can be compensated to some extent by a stabilization from a favorable metal–hydrogen interaction.

¹H NMR chemical shifts for structures **1a** and **1b** (M = Fe) were calculated and compared to experimental data.⁴ It is interesting that all ¹H chemical shifts calculated from the GIAO-B3LYP/II'/BP86/AE1^(*) method are underestimated (Table 2), i.e., calculated more upfield than the experimental shifts. The ratio between the calculated and experimental shifts ($\delta_{\text{cal}}/\delta_{\text{exp}}$) ranges from 0.88 to 0.99, with somewhat better agreement between calculated and experimental values for the *cis* isomer (**1a**).⁴¹ These results suggest that the calculated ¹H chemical shifts for ferrocenyl-type carbocations could be corrected by an appropriate scaling to obtain accurate chemical shifts, as suggested earlier.⁴² In addition we have calculated ¹H, ¹³C, and ⁵⁷Fe shifts for some representative ring-protonated (**3a** and **5a**)

(36) For comparison, the calculated WBI in the water dimer (H₂O···HOH) is only 2 times larger than the corresponding value in the structures **TS_{rot}** (M = Fe), but 2 times smaller than the corresponding value in **TS_{rot}** (M = Ru).

(37) In the case of (nonprotonated) formylferrocene and formylruthenocene the calculated energy barriers for the corresponding rotations are 8.1 and 8.8 kcal/mol, respectively, which is ca. 2 times lower as in the protonated forms (17.8 and 17.9 kcal/mol, respectively, see above). These values refer to structures for the formyl group rotation with the carbonyl group in an *endo* position; the corresponding transition structures with an *exo* carbonyl group were calculated to be ca. 1 kcal/mol less stable.

(38) The importance of electrostatic interaction effects on the decrease of the rotational barrier has recently been discussed; see: Baudry, J. *J. Am. Chem. Soc.* **2006**, *128*, 11088–11093.

(39) Harrington, L. E.; Vargas-Baca, I.; Reginato, N.; McGlinchey, M. J. *Organometallics* **2003**, *22*, 663–669, and references therein.

(40) Turbitt, T. D.; Watts, W. E. *J. Chem. Soc., Perkin Trans. 2* **1974**, 177–184.

(41) A similar value was calculated for the carbonyl-protonated forms of acetyl-ferrocenes (both *cis* and *trans* isomers).

(42) Siehl, H. U.; Vrček, V. In *Calculation of NMR and ESR Parameters. Theory and Applications*; Kaupp, M., Buhl, M., Malkin, V. G., Eds.; Wiley-VCH: Weinheim, 2004; pp 371–394.

(34) Vrček, V.; Bühl, M. *Organometallics* **2006**, *25*, 358–367.

(35) Wiberg, K. *Tetrahedron* **1968**, *24*, 1083–1096.

Table 2. Experimental and Calculated^a ¹H NMR Chemical Shifts of the Carbonyl- (**1a** and **1b**), Ring- (**3a** and **5a**), and Metal-Protonated (**9a**) Formylferrocenes, and Ferrocenylalkylium Ions **2** (R = H or Me)

	C5-H	C2-H	C4-H	C3-H	C α -H	(C1'-C5')-H	R ^b -H	Fe
exptl ^c	4.67	5.42	6.00	6.35	9.50	5.01		
1a	4.11	5.11	5.91	6.21	8.51	4.41	6.7	2416
1b	4.21	4.51	5.91	6.11	8.61	4.51	6.5	2159
3a	6.42	5.31	6.47	3.88	10.2	4.88	-2.56	1390
5a	5.13	6.75	5.18	4.4	10.16	4.88	-1.53	1225
9a	5.99	6.66	6.07	3.88	9.93	5.01	5.91	410
2 (R = H)	4.17	4.17	6.08	6.08	5.01	4.80		1292
exptl ^d	4.72	4.72	6.34	6.34	6.00	5.28		1015
2 (R = Me)	4.45	3.98	6.00	6.11	7.05	4.59	2.61	1644
exptl ^d	5.82	5.27	6.42	6.59	7.39	5.27	2.24	1319

^a GIAO-B3LYP//BP86 level, see Scheme 1 for atom numbering. ^b **1a** (R = O), **1b** (R = O), **3a** (R = C2), **5a** (R = C2'), **9a** (R = Fe), **2** (R = C β). ^c Protonated formylferrocene, from ref 4. ^d From ref 43.

and metal-protonated (**9a**) forms (for calculated ¹³C data see Supporting Information). As expected, discrepancies between the calculated and experimental ¹H values are even more evident (calculated values are more scattered in both directions) in case of these high-energy intermediates (Table 2).

We have also calculated chemical shifts for ferrocenylalkylium ions **2** (Scheme 1, R = H or Me), for which both ¹H and ⁵⁷Fe experimental data are available.⁴³ Again, all calculated ¹H chemical shifts are underestimated, as described above, while ⁵⁷Fe chemical shifts are overestimated, i.e., calculated more downfield than the experimental values.⁴⁴ However, the relative ⁵⁷Fe chemical shift difference on going from R = H to R = Me ($\Delta\delta_{\text{exp}} = 304$ ppm) is properly reproduced ($\Delta\delta_{\text{calc}} = 352$ ppm). A large range of ⁵⁷Fe chemical shifts (from 410 to 2416 ppm) is calculated for different protonated forms of formylferrocenes **1a–9a**, suggesting that ⁵⁷Fe NMR could be a sensitive tool to probe the preferred site of protonation.

3.2. Ring-Protonated Forms of Formylmetallocenes. In the temperature-dependent ¹H NMR spectra of protonated acylferrocenes, the cyclopentadienyl ring protons are notably deshielded at higher temperatures, suggesting that, in addition to the carbonyl oxygen protonation, higher lying C-ring protonated isomers may become populated to a significant extent.⁴⁵ Experimental data on the structures of such ring-protonated forms of acylferrocenes, however, are not available. We have located several ring-protonated formylferrocene forms **3a–6b** (Scheme 1), and all were found ca. 15–16 kcal/mol less stable than the carbonyl-protonated form **1** (M = Fe) at the BP86/AE1^(*) level (Table 1). All these structures are characterized by an agostic interaction, i.e., the presence of an intramolecular nonlinear C–H–Fe bond.

In addition, three symmetrical minima (C_s point group) were located with formyl groups orthogonal to the cyclopentadienyl ring, namely, protonated at C1 (**7a** and **7b**, R = H) or C1' position (**8**, Scheme 1). Interestingly, in structures **7a** and **7b** the two Cp moieties are staggered with respect to each other (not eclipsed, as usual).

The structures **7a** and **7b** (R = H) are of importance, as they represent possible intermediates in the *endo* mechanism of

electrophilic formylation of ferrocene. The analogous structures **7a** and **7b** (R = Me), protonated at C1 and with the acetyl group orthogonal to the Cp ring, could not be located as minima at the LDA (local density approximation) level.⁷ This has been taken as an indication that the *endo* mechanism of ferrocene acylation is not operative. However, when BP86 or B3LYP hybrid functionals are employed, structures **7a** and **7b** (R = Me) are characterized as stable minima. It appears that the LDA method is not sufficient to correctly describe stationary points on the corresponding potential energy surface. Our computational results suggest that both the *endo* and *exo* mechanism of ferrocene acylation could be operative.

Structures analogous to both **7a** and **7b** with an extra proton in an *endo* position (pertinent to an *exo* formylation of ferrocene) could not be located as minima. During a geometry optimization such structures converged to the most stable form of the metal-protonated formylferrocene **9a** (an *endo* proton is transferred from the C1 atom to the metal center). This suggests that an *exo* attack of the formyl cation to ferrocene is a barrierless process, at least in the gas phase, where a large driving force for the formation of **9a** from pristine ferrocene and CHO⁺ is computed (ΔG_{calc} for the modeled reaction ferrocene + CHO⁺ \rightarrow **9a** is -65 kcal/mol). Indeed, our attempts to locate an encounter complex between ferrocene and formyl cation positioned more than 3 Å above the Cp ring resulted again in **9a** (Scheme 1). This metal-protonated form could be easily rearranged to the more stable oxygen-protonated form **1b**, thus completing a continuous path for *exo* attack of a HCO⁺, mimicking Friedel–Crafts acylation. The transition state **TS_{1b,9a}** for this intramolecular rearrangement **9a** \rightarrow **1b** is located and characterized by a relatively large imaginary frequency (976i cm⁻¹), which corresponds to the proton shift from the iron center to the oxygen. It is calculated to be 5.1 kcal/mol less stable than **9a** (Figure 1).

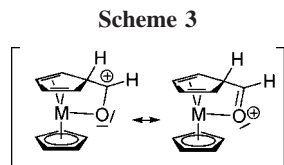
Structure **7b** (M = Fe, R = H) is characterized by a weak interaction between the metal center and the aldehyde H atom and is very high in energy (more than 30 kcal/mol above **1a**) due to the loss of resonance energy upon protonation at C1. Both **7a** and **8** are more stable than **7b** and are calculated to be only slightly higher in energy than the other ring-protonated forms **3a–6b** (see Scheme 1 and Table 1). **7a** is stabilized by a strong interaction between the carbonyl O atom and the metal center. The presence of a BCP between these two atoms with large values of 0.073 and 0.422 au for the electron density (ρ) and its Laplacian ($\nabla^2\rho$), respectively, is indicative of an intramolecular coordinative bond between iron and oxygen atoms and suggests a saturated 18-e configuration of **7a** (as depicted in Scheme 3).

The calculated Wiberg bond index for this Fe–O bond is 0.329, which is in the range (from 0.260 to 0.470) of calculated

(43) For experimental ¹H and ¹³C chemical shifts of **2** see: (a) Ceccon, A.; Giacometti, G.; Venzo, A.; Paolucci, D.; Benozzi, D. *J. Organomet. Chem.* **1980**, *185*, 231–239. For experimental ⁵⁷Fe chemical shifts of **2** see: (b) Benn, R. In *Transition Metal Nuclear Magnetic Resonance*; Pregosin, P. S., Ed.; Elsevier: Amsterdam, 1991; pp 103–142. (c) Koridze, A. A.; Stakhova, N. M.; Petrovskii, P. V. *J. Organomet. Chem.* **1983**, *254*, 345–360.

(44) A similar result was obtained for **2** (R = H) at the B3LYP/6-311+G** level: Wrackmeyer, B.; Tok, O. L.; Koridze, A. A. *Magn. Reson. Chem.* **2004**, *42*, 750–755.

(45) As well, O-protonation of phenol and anisole was observed at low temperature, while C-protonation was found at higher temperatures: Olah, G. A.; Mo, Y. K. *J. Org. Chem.* **1973**, *38*, 353–366.



values for Fe–C coordinative bonds (except for the Fe–C1, which is as low as 0.020). The coordination of the carbonyl oxygen to the iron center has been recently described as an unusual interaction in ferrocene chemistry⁴⁶ and is also related to numerous examples where both ketones and aldehydes are interacting with different metal centers (M = Fe, Ru, Re, . . .) in various organometallic complexes.⁴⁷

Interestingly, the *endo* H atom at C1' in **8** (R = H) is involved in interactions with both the iron and oxygen atom. This is apparent from topological analysis, which indicates the existence of bifurcated bond paths or three-center hydrogen bonds involving these three atoms. The BCPs connecting the C1'-hydrogen with iron and oxygen are characterized by ρ values of 0.093 and 0.024 au, respectively, and by $\nabla^2\rho$ of 0.205 and 0.055 au, respectively. According to these results structure **8** can be classified as an unusual compound with an unsymmetrical three-center hydrogen bridge acting as H-bond donor.⁴⁸ There is also a BCP between Fe and C1' atoms ($\nabla^2\rho$ 0.304 and ρ 0.089 au), suggesting another bifurcated interaction (O–Fe–C1') in this nonconventional structure **8** (R = H or Me). Moreover, the formation of such an intermediate in which the acyl backbone is orthogonal to the Cp ring and the oxygen atom points toward the metal-bonded proton is considered a driving force for an *exo* acylation of ferrocene.⁷

No C1- or C1'-protonated minimum with the formyl group coplanar to the Cp ring could be located. A corresponding C1'-protonated structure (analogous to **8**, but with a rotated formyl group) converged to the C2'-protonated minimum **5a** upon optimization. Attempted optimization of a C1-protonated structure (**7a/b** with rotated formyl groups) yielded a new structure, **7c** (R = H, Scheme 1), in which the iron atom is bonded to the formyl group. The calculated bond distance between Fe and the C(carbonyl) atom is only 2.109 Å and is characterized by a BCP ($\nabla^2\rho = 0.113$ and $\rho = 0.0889$ au) very similar to other Fe–C(Cp) bonds in **7c**, while the calculated WBI for this Fe–C(carbonyl) bond is even larger (0.454 Å) if compared to other Fe–C(Cp) bonds (ranging from 0.261 to 0.306 Å). The metal-bonded formyl group is coplanar with respect to two Cp rings, while the corresponding structure with the orthogonal formyl group was not located as a minimum. Analogously to **7a** and **7b**, the structure **7c** (R = H or Me) is also related to the *endo* mechanism of the ferrocene acylation (see above). It can be assumed as an intermediate product of the precomplexation step between ferrocene and the acyl-cation during an *endo* acylation process.⁷ Geometry optimizations of ferrocene and the formyl cation positioned between the two Cp rings and separated by more than 4 Å from the metal center resulted in formation of **7c**, suggesting that an *endo* attack of HCO⁺ leads first to the metal- and not a ring-formylated product. The calculated Gibbs energy of the separated forms (see Supporting

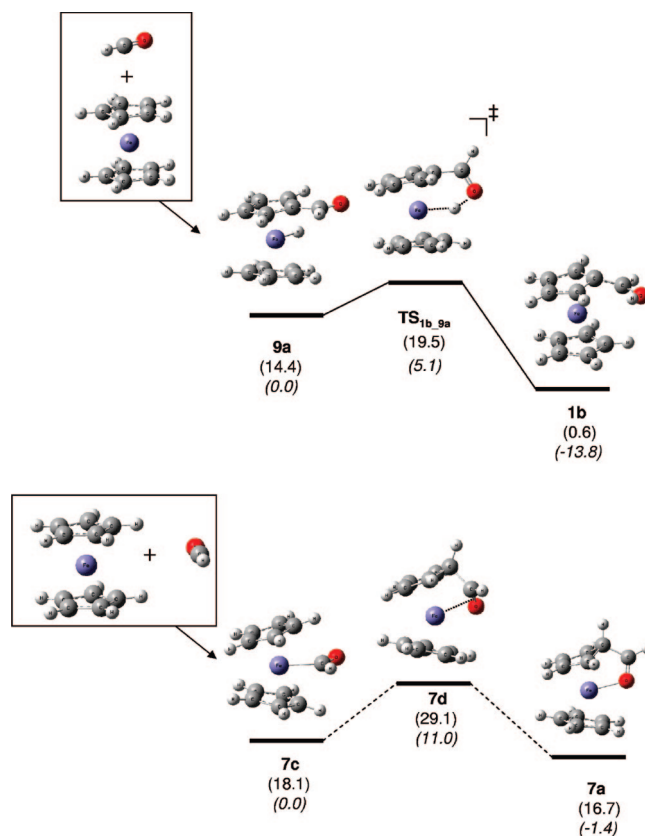


Figure 1. Key stationary points during attack of a model electrophile, HCO⁺, on ferrocene (in parentheses: energies in kcal/mol relative to **1a**; *in italics*: relative to initial product). Arrows indicate barrierless relaxation during geometry optimization from the starting configurations in the boxes. Top: *exo* pathway; bottom: *endo* pathway.

Information), i.e., ferrocene and a naked formyl cation itself, is more than 60 kcal/mol higher than that of **7c** in the gas phase.

Attempts to locate a transition state leading directly from **7c**, the presumed initial product during *endo* attack of HCO⁺, to **7a** via transfer of the formyl group from iron to a Cp-carbon atom, were unsuccessful so far. In the course of this search another minimum was located, **7d** (Scheme 1), in which the carbonyl group is attached in a “side-on” fashion to the metal, rather than “end-on” via the O atom as in **7a**. This side-on form **7d** could be a plausible intermediate on the route from **7a** to **7c**, because it contains a C(Cp)–C(carbonyl) bond as in **7a**, as well as a Fe–C(carbonyl) contact as in **7c**. **7d** is computed to be 11.0 kcal/mol higher in energy than **7c**. The actual reaction barriers will be even higher,⁴⁹ so that the *endo* attack of HCO⁺ appears to be much less favorable than the *exo* route, which proceeds smoothly via **9a** (see above). At least with this model electrophile, Friedel–Crafts acylation of ferrocene is thus predicted to proceed swiftly via an *exo* pathway. These findings are summarized pictorially in Figure 1.

No ring-protonated minima were found for ferrocenylruthenocene, except for the two structures **7a** and **7b** (Scheme 1, M = Ru). However, when using a higher basis set (6-311+G** on C and O atoms) or better grid size (ultrafine), these structures were characterized as first-order stationary points. All other

(46) Kilner, C. A.; Halcrow, M. A. *Acta Crystallogr.* **2006**, C62, m437–m439.

(47) See for example: (a) Klein, D. P.; Quiroz Mendez, N.; Seyler, J. W.; Arif, A. M.; Gladysz, J. A. *J. Organomet. Chem.* **1993**, 450, 157–164. (b) Hamon, P.; Toupet, L.; Hamon, J.-R.; Lapinte, C. *J. Chem. Soc., Chem. Commun.* **1994**, 93, 1–932. (c) Costes, J.-P.; Clemente-Juan, J. M.; Dahan, F.; Dumestre, F.; Tuchagues, J.-P. *Inorg. Chem.* **2002**, 41, 2886–2891.

(48) Rozas, I. *Phys. Chem. Chem. Phys.* **2007**, 9, 2782–2790, and references therein.

(49) Despite extensive searches, we were not able to locate a transition state between **7c** and **7d**. That between **7d** and **7a** could be found and is only 0.1 kcal/mol above **7d** on the potential energy surface at the BP86/AE1(*) level.

starting geometries (protonated at any ring position) converged to the more stable metal-protonated form (see below) or to the ruthenium-formylated structure **7c** (Scheme 1).

3.3. Metal-Protonated Forms of Formylmetalocenes.

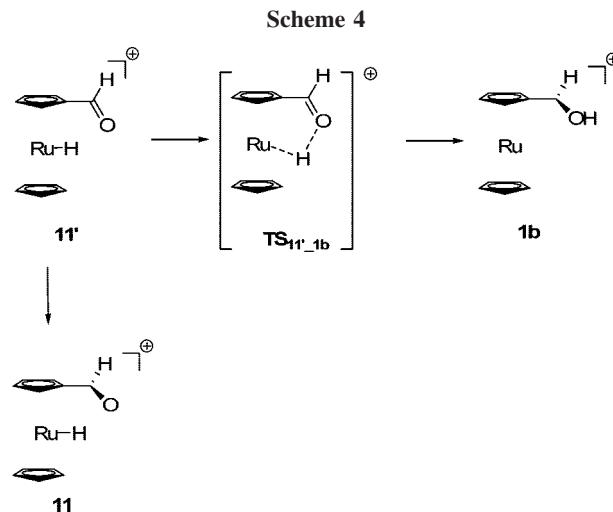
There is no direct experimental evidence for protonation of the iron atom in acylferrocenes, but it has been suggested⁴ that such iron-protonated acylferrocenes could be stabilized by hydrogen bonding (Scheme 1) or by some other type of intramolecular interaction. Imposing C_s symmetry, a stationary point with such an interaction can be located (**11'** in Scheme 1, M = Fe), but this is a transition state for rotation of the formyl group, in order to restore conjugation with the Cp moiety.

At the BP86/AE1(*) level four metal-protonated minima could be located (**9a–10b** in Scheme 1), which are all 14–16 kcal/mol above the global minimum **1** (M = Fe), i.e., in the same energy range as the ring-protonated forms **3a–6b** (Table 1). A comparable stability of iron- and ring-protonated (or agostic) structures has also been obtained at similar levels for protonated ferrocene itself.² However, at the B3LYP/AE1(*) level of theory all metal-protonated structures converged to the more stable ring-protonated forms, which is in agreement with earlier findings for ferrocene that ring protonation is more favorable than metal protonation by ca. 2 kcal/mol with B3LYP.² Consistent with findings that it is energetically unfavorable for a –CHO substituent to reside in the “pinch position”,⁵⁰ structure **11**, with an Fe–H bond positioned between C1 and C1', converged to the monoprotonated ring-protonated form **5a** during geometry optimization.

For protonated formylruthenocene (M = Ru, Scheme 1) all five metal-protonated forms (**9a**, **9b**, **10a**, **10b**, **11**) were located as stable minima. On average, the metal-protonated formylruthenocenes are less stable than the carbonyl-protonated forms by 12.5 kcal/mol. We were not able to locate any ring-protonated formylruthenocene minimum at the BP86/ECPI(*) level.⁵¹ Likewise, for the parent protonated ruthenocene itself only a metal-protonated minimum could be located at that level.⁵²

Therefore, in the formylruthenocene series the site of protonation is either on the metal center or on the oxygen atom of the formyl group. In contrast, in the formylferrocene series ring protonation is an energetically more feasible process than metal protonation. Similar results are obtained for the corresponding metallocenyl-alcohols and -ethers.⁵³

The minimum of type **11**, not located in the case of M = Fe, can be found for M = Ru, but is ca. 1.7 kcal/mol less stable than structures **9a–10b**. Structure **11'**, with the formyl group orthogonal to the cyclopentadienyl ring (Scheme 1, M = Ru), is a true minimum as well. This minimum is characterized by an elongated Ru–H bond (1.609 Å), as compared to **9a–11** (1.589 Å, on average), by a fairly short O···H distance (2.054 Å), and by a BCP between H and O ($\rho = 0.026$ au, $\nabla^2 \rho = 0.065$ au), all consistent with the presence of a Ru–H···O hydrogen bond. Since **11'** is calculated to be 0.5 kcal/mol more stable than **11**, the loss of resonance energy due to the rotation about the C1–C(carbonyl) bond is compensated by the energy gain from formation of the intramolecular hydrogen bond in **11'**. Apparently, **11'** and **8** are the only minima among all



protonated formylmetalocenes, in which the formyl group is oriented orthogonally relative to the cyclopentadienyl ring.

The Ru-protonated structure **11'** is easily converted into the more stable carbonyl-protonated form **1b** by an intramolecular proton transfer from the ruthenium to the carbonyl oxygen atom (Scheme 4). This process involves a transition structure **TS_{11'_1b}**, which is characterized by a single imaginary frequency ($-713i$ cm^{-1}) corresponding to the H shift between Ru and O atoms. This transition state is calculated to be only 4.8 kcal/mol above **11'**, a rather low barrier for a proton transfer.

We have also investigated the mechanism of interconversion between the Ru-protonated isomers **9a–11**. To this end, we have located four transition state structures along the sequence **9a** \rightleftharpoons **10a** \rightleftharpoons **10b** \rightleftharpoons **9b** \rightleftharpoons **11** (see Supporting Information).

Every transition state structure is characterized by a rather low imaginary frequency (ranging from $46i$ cm^{-1} for **TS_{10b_9b}** to $53i$ cm^{-1} for **TS_{9b_11}**), which corresponds to simultaneous movement of the ruthenium-bonded proton and one of the Cp rings. All these transition states are computed to be 3–6 kcal/mol above **9a**, the most stable metal-protonated formylruthenocene,⁵⁴ but of comparable (or lower than) energy to **TS_{11'_1b}**. Thus, the highest point on the potential energy surface that has to be passed in order to reach and scramble all the metal-protonated isomers is 15.0 kcal/mol above the global minimum **1a**. Such a barrier would imply that fluxional processes involving these metal-protonated intermediates are feasible even at ambient temperatures, albeit, presumably, at a rather low rate.

As expected, the computed proton affinities (PAs) of formylferrocene and formylruthenocene yielding **1a**, 229.4 and 224.2 kcal/mol for M = Fe and Ru, respectively [BP86/AE1(*) level], are significantly higher than that of ferrocene, 214.4 kcal/mol at the same level.⁵⁵ The difference between the PAs of ferrocene and the formylmetalocenes reflects the stabilization of the O-protonated forms **1a/1b** with respect to the corresponding ring- or metal-protonated isomers (Table 1).

To summarize this part, even though the oxygen-protonated formylruthenocenes **1a** and **1b** will be by far the predominant

(50) Bitterwolf, T. E.; Campbell Ling, A. *J. Organomet. Chem.* **1972**, *40*, 197–203.

(51) The same was found with B3LYP and BLYP models, using either ECPI* or a more extended basis set.

(52) In an earlier theoretical study with small basis sets (BLYP/LANL2DZ), also ring-protonated structures can be found for protonated ruthenocene; cf. Borisov, Y. A.; Ustyniuk, N. *A Russ. Chem. Bull.* **2002**, *51*, 1900–1908.

(53) Vrčec, V.; Bühl, M. Unpublished results.

(54) For the oxygen-protonated minimum **1b**, the energy barriers for Cp ring rotations are much smaller, less than 1 kcal/mol.

(55) (a) 211.0 kcal/mol at B3LYP/AE1(*). Experimental numbers for the PA of ferrocene vary between ca. 207 kcal/mol (Meot-Ner, M. *J. Am. Chem. Soc.* **1989**, *111*, 2830–2834) and 210 kcal/mol. (b) (as cited in: Jolly, W. L. *Modern Inorganic Chemistry*, 2nd ed.; McGraw-Hill: New York, 1991). (c) For selected computational studies of this quantity see e.g.: McKee, M. L. *J. Am. Chem. Soc.* **1993**, *115*, 2818–2824. (d) Mayor-López, M. J.; Lüthi, H. P.; Koch, H.; Morgantini, P. Y.; Weber, J. *J. Chem. Phys.* **2000**, *113*, 8009–8014. (e) Hyla-Krispin, I.; Grimme, S. *Organometallics* **2004**, *23*, 5581–5592.

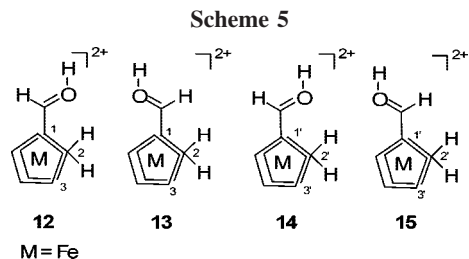


Table 3. Calculated^a ¹H NMR Chemical Shifts (in ppm relative to TMS) of Diprotonated Formylferrocenes **12–15**

	(C2,C5)–H	(C3,C4)–H	C α –H	(C1'–C5') _{av} –H	O–H	H _{extra}
expt ^b	7.6	7.2	10.5	6.5	14.2	–2.7
12	6.8	6.9	9.1	5.5	10.0	–3.8
13	6.9	6.8	8.6	5.5	10.0	–3.4
14	6.6	6.5	9.1	5.5	10.2	–2.1
15	6.6	6.3	9.3	5.5	10.1	–2.0

^a GIAO-B3LYP/II//BP86/AE1^(*) level, see Scheme 5 for atom numbering. ^b From ref 56.

constituents of the equilibrium mixture, metal-protonated isomers could be accessible under ambient conditions.

3.4. Diprotonated Forms of Formylferrocene. In addition to monoprotonated acyl-ferrocenes, diprotonated species, for which experimental results exist,⁵⁶ were calculated as well. While the first protonation always occurs at the carbonyl oxygen atom, the second protonation must occur either at the metal center or at one of the ring carbon atoms. This question was addressed by Sommer et al. by using stronger superacids, and they have concluded that the second protonation occurs on the central metal atom.⁵⁵ In searching for all diprotonated minima, we have found that structures **12–15** (Scheme 5) are the most stable (all are calculated in the small energy range of ca. 1.5 kcal/mol, see Supporting Information). These structures are protonated at both the oxygen (*cis*-orientation) and carbon atom (either C2 or C2'). In contrast to previous interpretations of the experimental findings, all structures protonated at both oxygen and iron atoms converged, during geometry optimization, to one of the corresponding minima **12–15**. In the latter, the calculated Fe–H distances (ranging from 1.626 to 1.650 Å) are noticeably longer than the corresponding Fe–H bonds in monoprotonated species **9a–10b** (which range from 1.499 to 1.503 Å). In addition, in **12–15** the extra proton at the metal is rather close to the nearest C atom of the Cp moiety (1.30 Å, on average), which makes these structures similar to those of the ring-protonated forms **3** and **5** (Scheme 1, M = Fe), where the average C–H bond distance is calculated slightly over 1.35 Å, or to those of ring-protonated (or agostic) ferrocene itself.²

We have also calculated ¹H NMR chemical shifts for structures **12–15** and found good agreement with experimental data (Table 3). Interestingly, the experimental high-field shift of the second extra proton ($\delta_{\text{exp}} = -2.7$ ppm) is well reproduced when an averaged ¹H chemical shift for **12–15** is considered (calculated $\delta_{\text{av}} = -2.8$ ppm).⁵⁷ Given the potential sensitivity

(56) Rimmelin, P.; Sommer, J.; Sandström, J.; Seita, J. *J. Organomet. Chem.* **1976**, *114*, 175–177.

(57) On the basis of the relative energy differences between the diprotonated formyl-ferrocenes (isomers **12–15** are calculated to be 5–17 kcal/mol more stable than other diprotonated species), one can estimate that contributions of other diprotonated species to the averaged chemical shifts of ferrocenylmethanol are relatively small.

of the results on details of the computational methodology (cf. protonated ferrocene),² this degree of agreement should probably not be overinterpreted. However, the results are consistent with previous DFT studies of protonated ferrocene, which agree that truly metal-protonated minima should be associated with a strong deshielding of this extra proton and that negative upfield shifts, i.e., negative values, for this resonance are characteristic for agostic structures.^{2,58} We therefore propose to interpret the experimental results^{4,55} such that the second protonation of formylferrocene occurs at the carbon atom (either C2 or C2') of the Cp ring, not at the iron center as suggested earlier.⁵⁶

4. Conclusion

We have presented a computational study of protonated formylferrocene and formylruthenocene, charting large areas of their rich potential-energy landscapes. In agreement with experiment, the most stable form in each case is protonated at the formyl oxygen atom, with the proton *trans* to the metallocenyl moiety. According to computed rotational barriers in the –C α HOH side chain, conjugation between the π -system of the metallocenyl moiety and the C α atom is much more important than that between C α and the p-type lone pair at the O atom.

For formylferrocene, a plethora of additional metal- or ring-protonated (or agostic) isomers can be located, but these are all higher in energy by at least 14 kcal/mol. Isomers of this type are indicated to be important intermediates during Friedel–Crafts acylation of ferrocene, at least in the idealized case of free CHO⁺ as model electrophile. For this model, optimizations of salient stationary points furnish further support for the mechanistic picture that the incoming electrophile prefers an *exo* versus an *endo* attack. In the case of formylruthenocene, no ring-protonated or agostic species are found, and metal-protonated isomers are predicted to be ca. 10 kcal/mol less stable than the O-protonated minima. For doubly protonated formylferrocene, in contrast, no metal-protonated minimum can be located at all, and the second proton is predicted to be attached to one of the rings, with an agostic interaction to the metal. This structural assignment is supported by the good agreement between computed and experimental ¹H NMR chemical shifts.

Acknowledgment. M.B. wishes to thank Prof. W. Thiel and the Max-Planck-Institut für Kohlenforschung for continuing support. A Humboldt fellowship for V.V. is gratefully acknowledged. Computations were performed on Compaq XP1000 and ES40 workstations as well as on an Intel Xeon PC cluster at the MPI Mülheim. A.S. thanks the Computing Center of the University of Zagreb SRCE for allocating computer time on the Isabella cluster.

Supporting Information Available: Tables with additional energetic and NMR data, as well as BP86-optimized Cartesian coordinates of all complexes. This material is available free of charge via the Internet at <http://pubs.acs.org>.

OM700916F

(58) Karlsson, A.; Broo, A.; Ahlberg, P. *Can. J. Chem.* **1999**, *77*, 628–633.